Toxicology Reports 2 (2015) 341–350

Contents lists available at ScienceDirect

Toxicology Reports

journal homepage: www.elsevier.com/locate/toxrep

Toxicogenomic study in rat thymus of F1 generation offspring following maternal exposure to silver ion

Xiugong Gao*, Jeffrey J. Yourick, Vanessa D. Topping, Thomas Black, Nicholas Olejnik, Zachary Keltner, Robert L. Sprando

Division of Toxicology, Office of Applied Research and Safety Assessment, Center for Food Safety and Applied Nutrition, U.S. Food and Drug Administration, Laurel, MD, USA

ARTICLE INFO

Article history:
Received 11 December 2014
Accepted 11 December 2014
Available online 19 December 2014

Keywords:
Silver ion
Silver acetate
Maternal exposure
Rodent model
Toxicogenomics
Microarray
Thymus
Developmental toxicity

ABSTRACT

Male and female rats (26-day-old) were exposed to 0.0, 0.4, 4 or 40 mg/kg body weight silver acetate (AgAc) in drinking water for 10 weeks prior to and during mating. Sperm-positive females remained within their dose groups and were exposed to silver acetate during gestation and lactation. At postnatal day 26, the effect of silver ions on the developing F1 generation rat thymus was evaluated at the transcriptional level using whole-genome microarrays. Gene expression profiling analyses identified a dozen differentially expressed genes (DEGs) in each dose group using a loose criterion of fold change (FC) >1.5 and unadjusted $p < 0.05$, regardless of whether the analysis was conducted within each gender group or with both gender groups combined. No dose-dependent effect was observed on the number of DEGs. In addition, none of these genes had a false discovery rate (FDR) <0.05 after correction for multiple testing. These results in combination with the observation that thymus-to-body-weight ratios were not affected and no histopathological abnormalities were identified indicate that *in utero* exposure to silver ions up to 26.0 mg/kg (equivalent to 40.0 mg/kg silver acetate) did not have an adverse effect on the developing thymus.

1. Introduction

Silver has been used for centuries as a biocidal material. In ancient time, silver was used to preserve water in the form of silver vessels or silver coins. Its medical use was documented as early as 750 AD. Starting from the seventeenth century, silver has been used as antiseptics in a number of medical situations such as cholera, eye infection, and burn wound [2]. The U.S. Food and Drug Administration (FDA) approved the use of charged silver solutions (*i.e.* electrocolloidals) as antibacterial agents in the 1920s. The application of silver was further expanded during the second half of the twentieth century as a disinfectant in conjunction with hydrogen peroxide.

Today, silver-containing products are used in a wide range of healthcare, food industry, and domiciliary applications and are commonly found in hard surface materials and textiles. In the food industry, silver-containing compounds or their mixtures are widely applied onto food-packaging materials, often in direct contact with the food. Such an extensive use of silver raises concerns about its safety, toxicity, and health risk. However, there is a paucity

Abbreviations: AGCC, Affymetrix GeneChip Command Console; AgAc, silver acetate; AgNP, silver nanoparticle; DEG, differentially expressed gene; FC, fold change; FDR, false discovery rate; HCA, hierarchical cluster analysis; NOEL, no observed effect level; NK, natural killer; PCA, principal components analysis; RMA, robust multi-array average; SV, source of variance.

* Corresponding author at: 8301 Muirkirk Road, Laurel, MD 20708, USA. Tel.: +1 301 796 0580.
E-mail address: xiugong.gao@fda.hhs.gov (X. Gao).

http://dx.doi.org/10.1016/j.toxrep.2014.12.008

of information on the toxicity of silver. It is well known that ingesting large amount of silver preparations, which rarely happens, results in argyria, manifested by an irreversible gray to blue-black coloring of the skin due to subdermal silver deposit [11]. Also, the use of ionic silver and silver derivatives for treatment and prevention of infection of burn wounds or skin grafting has been associated with a number of side effects such as cytotoxicity, staining, methaemoglobinaemia and electrolyte disturbance, longer slough separation time, retardation of wound healing, and the possible inactivation of enzyme debriding agents [4]. The free silver ion (Ag^+) is the most toxic species of silver. Toxicity testing in fathead minnow (*Pimephales promelas*) showed that free silver ion was about 15,000 and 300 times more acutely toxic than silver sulfide and silver chloride complexes, respectively, which are the major forms of silver in the environment [9]. However, the toxic effect of long-term exposure to low concentrations of silver has not been well studied.

There is a potential risk for the developing fetus when pregnant women are exposed to silver products. A case–control epidemiology study was conducted by [1] among women who delivered infants from 1977 to 1980 in a Massachusetts hospital. Trace element levels of public water were analyzed from the communities in which the women resided during pregnancy. The relationship between community drinking water quality and the occurrence of late adverse pregnancy outcomes was examined. After adjustment for confounding factors, the results suggested some association between maternal exposures to 0.001 mg/L of silver in the drinking water (1/100 of the EPA standard) and some increase in fetal developmental anomalies (ear, face, and neck). As the authors recognized, there are inferential limitations to epidemiologic studies and further research is needed to explore these findings.

The U.S. FDA evaluated data available on the use of silver mixtures as antimicrobial agents in food contact polymers and suspected that *in utero* exposure to silver may have an adverse effect on the immune system of the developing animal. A comprehensive study for risk assessment has been conducted in our group using a rat model and conventional toxicological and/or pathological endpoints to confirm that the previously observed adverse effects are due to silver ion alone, and to define the no observed effect level (NOEL) at or below which the adverse effect does not occur [16].

Microarray technology has become a powerful tool to explore the expression levels of thousands of genes or even complete genomes after exposure to toxicants and has thus found wide applications in toxicological research [15]. Toxicogenomics, defined as the "global analysis of gene expression in target cells or tissues in response to a toxicant," has emerged as a promising approach to evaluate mechanisms of action in toxicological models [5]. Information on the global gene expression profile may provide clues to understanding biological actions of toxic substances at the molecular, cellular, tissue, and individual animal levels. Tissue-specific gene expression profiles can provide a basis for understanding tissue function, enabling molecular characterization of differences between normal and diseased tissue. Toxicogenomics also provides opportunities for improvements in toxicity screening and risk assessment such as the development of new predictive models for identifying human health hazards and the identification of more precise molecular biomarkers of exposure [12]. In this application, toxicogenomic approaches usually are more sensitive than conventional toxicological endpoint assays and can assess toxic responses at low doses and at the very onset.

As a component of the comprehensive research [16], the current study used a toxicogenomic approach to study the effect of silver ions on the developing thymus at the transcriptional level by using whole-genome microarrays to study global gene expression changes in rat thymus of F1 generation offspring from dams exposed to different levels of silver ion. In the last years, some dozen reports appeared in the literature using toxicogenomics approach to study silver toxicity; however, the majority of these studies were on silver nanoparticles (AgNPs). Only a few evaluated silver ion toxicity either in a crustacean model [13], an *in vitro* fish model [20], or in bacteria [21]. Silver ions and AgNPs exerted toxicity through different mechanisms; the latter was affected by several other factors other than silver ion itself, including surface coating and particle size [13]. To our knowledge, this study represents the first evaluation of silver ion toxicity using toxicogenomics approach in a mammalian model.

2. Materials and methods

2.1. Experimental design

Thymus tissues were obtained from 5 male and 5 female F1 generation rat pups on postnatal day 26 in each treatment group that were randomly selected from the animals evaluated in [16]. In brief, 28-day-old male and female CD IGS VAF/+ rats were exposed *ad libidum* to Hydro-System water containing 0 (control), 0.4, 4.0, or 40.0 mg/kg body weight silver acetate for 10 weeks prior to mating and during the 2–3 week mating period. Sperm-positive females remained within their dose groups and were further exposed to silver acetate throughout the gestation and lactation periods. Pups were weaned on lactation day 21 and euthanized for tissue collection on day 26. To minimize potential litter effect, no more than one pup was randomly selected from each litter within a treatment group.

2.2. Tissue collection, RNA isolation, and quality assurance

Thymus from each pup was collected and snap-frozen in liquid N_2 with 5 min after dissection. The samples were kept in a −80 °C freezer until processing for total RNA extraction. Thymus was disrupted using the TissueLyser (Qiagen, Valencia, CA) in the QIAzol Lysis Reagent (Qiagen) and total RNA was isolated on the EZ1 Advanced XL (Qiagen) automated RNA purification instrument using the EZ1 RNA Universal Tissue Kit (Qiagen) following the manufacturer's protocol, including an on-column DNase digestion. RNA concentration and purity (260/280 ratio) were measured with the NanoDrop ND-1000 spectrophotometer (NanoDrop Technologies, Wilmington, DE). Integrity of RNA samples was assessed by the Agilent 2100 Bioanalyzer

(Santa Clara, CA) with the RNA 6000 Nano Reagent Kit from the same manufacturer.

2.3. Microarray experiment

The total RNA samples were preprocessed for hybridization to GeneChip Rat Genome 230 2.0 Array (Affymetrix, Santa Clara, CA) using the Affymetrix GeneChip 3′ IVT Express Kit following the manufacturer's protocol. In brief, 0.1 μg of total RNA was used to generate first-strand cDNA using reverse transcriptase and a T7-linked oligo(dT) primer. After second-strand synthesis, the double-stranded cDNA was then used for *in vitro* transcription with biotinylated UTP and CTP to amplify the product, referred to as cRNA amplification. Subsequent hybridization, wash, and staining were carried out using the Affymetrix GeneChip Hybridization, Wash, and Stain Kit and the manufacturer's protocols were followed. Briefly, biotinylated target cRNA was fragmented using heat and Mg^{2+} to sizes of 35–200 bp. Each fragmented cRNA target sample (approximately 12.5 μg) was individually hybridized to a GeneChip Rat Genome 230 2.0 Array at 45 °C for 16 h in Affymetrix GeneChip Hybridization Oven 645. After hybridization, the array chips were stained and washed using an Affymetrix Fluidics Station 450. The chips were then scanned on Affymetrix GeneChip Scanner 3000 7G and the image (.DAT) files were preprocessed using the Affymetrix GeneChip Command Console (AGCC) software v.3.2 to generate cell intensity (.CEL) files. The Rat Genome 230 2.0 Array comprises of over 31,000 probe sets representing approximately 28,700 well-substantiated rat genes. Prior to data analysis, all arrays referred to in this study were assessed for data quality using the Affymetrix Expression Console software v.1.2 and all quality assessment metrics (including spike-in controls during target preparation and hybridization) were found within boundaries.

2.4. Data processing and statistical analysis

Data analysis was carried out primarily using the U.S. FDA's ArrayTrack software system [17,18]. The values of individual probes belonging to one probe set in .CEL files were summarized using the robust multi-array average (RMA) algorithm [8] embedded in ArrayTrack, which comprises of convolution background correction, quantile normalization, and median polish summarization. Normalized data for all samples were then analyzed by unsupervised principal component analysis (PCA) [14] and hierarchical cluster analysis (HCA) [3], both embedded in ArrayTrack, to identify patterns in the dataset and highlight similarities and differences among the samples. Subsequently, differentially expressed genes were selected using one-way analysis of variance (ANOVA) based on Welch's *t*-test. To improve moderated *t*-statistics, a gene-filtering procedure, namely I/NI-calls [6], was applied before the Welch's *t*-test to exclude non-informative genes. For each comparison between two experimental groups, the fold change (FC) of every annotated gene, together with their corresponding *p*-value, was used for selection of differentially expressed genes with cutoffs of $p < 0.05$ and FC > 1.5.

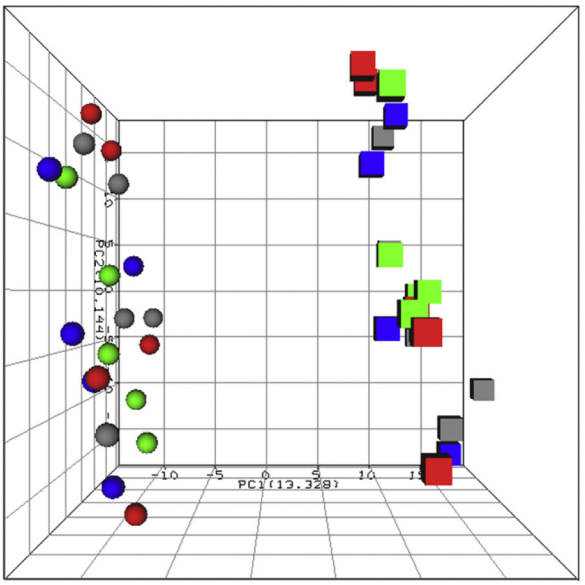

Fig. 1. Principal component analysis based on all probe sets in the array to cluster samples based on their similarities or dissimilarities in global gene expression level. The shape of each sample represents gender with male samples as cubes and females as balls. The color represents different treatment groups: grey, group 1 (control); green, group 2 (0.4 mg/kg); blue, group 3 (4.0 mg/kg); red, group 4 (40.0 mg/kg). The three axes PC1, PC2, and PC3 represent the first three principal components identified by the analysis. The percentage contribution of each component to the overall source of variation is included in the parentheses following each component name. The first principal component (PC1), which separates the samples into two gender clusters, has the largest variance (13.328), followed by PC2 (10.144) and PC3 (4.839).

3. Results

3.1. Thymus and body weights

Table 1 summarizes the effects of silver acetate on rat thymus and body weights in the subset of F1 generation pups used in this study (the full animal dataset was previously reported by [16]). Despite some decreases in the mean thymus and body weights in the higher dosing groups (4.0 and 40.0 mg/kg) compared with the control animals, thymus/body weight ratios were similar in all groups. No statistically significant effects were seen in any group.

3.2. Global gene expression profiling

Unsupervised data exploration by principal components analysis (PCA) was first conducted to identify major effects influencing the expression values in the experiment and to cluster samples based on their similarities or dissimilarities in global gene expression level. As shown in Fig. 1, overall the samples were separated by gender into two major clusters. With each gender cluster, samples of different treatment groups were mixed with no discrete boundaries between different groups, suggesting treatment by silver acetate had little effect on global gene expression level. Results of hierarchical cluster analysis (HCA) (Fig. 2) are consistent with the PCA results. The samples were clustered by gender into two major branches;

Table 1
Summary of thymus and body weights and their ratios.

		Thymus Weight (mg)[a]	Body Weight (g)	Thymus/Body Ratio (mg/g)
Group 1 (Control)	Male (5)[b]	302.9 ± 50.3	86.3 ± 4.8	3.5 ± 0.5
	Female (5)	332.5 ± 14.3	81.5 ± 3.3	4.1 ± 0.3
	All (10)	317.7 ± 38.2	83.9 ± 4.6	3.8 ± 0.5
Group 2 (0.4 mg/kg)	Male (5)	307.1 ± 62.2	86.7 ± 7.2	3.5 ± 0.6
	Female (5)	343.9 ± 95.7	81.3 ± 12.1	4.2 ± 0.7
	All (10)	325.5 ± 78.5	84.0 ± 9.8	3.9 ± 0.7
Group 3 (4.0 mg/kg)	Male (5)	304.9 ± 45.4	78.2 ± 4.2*	3.9 ± 0.7
	Female (5)	280.5 ± 29.6**	74.1 ± 5.2*	3.8 ± 0.4
	All (10)	292.7 ± 38.3	76.1 ± 5.0**	3.9 ± 0.5
Group 4 (40.0 mg/kg)	Male (5)	273.1 ± 54.8	76.7 ± 7.9*	3.5 ± 0.4
	Female (5)	262.4 ± 58.6*	71.2 ± 8.2*	3.7 ± 0.7
	All (10)	267.7 ± 53.8*	74.0 ± 8.1**	3.6 ± 0.6

[a] Thymus was weighed after frozen in liquid nitrogen.
[b] The number in parentheses indicates the number of animals in each dose and sex group.
* Significant at $p < 0.05$.
** Significant at $p < 0.01$.

within each gender cluster, however, the samples were not clustered into different treatment groups. Instead, the samples formed branches with no apparent relationships.

3.3. Differential gene expression in treatment groups

Differences in gene expression between the treatment groups and the control were assessed using one-way analysis of variance (ANOVA). Since each gender had a distinct pattern in global gene expression (Figs. 1 and 2), the analysis was conducted either separately for female and male animals, or with all animals in the same dose group.

Consistent with the results from PCA and HCA (Figs. 1 and 2), one-way ANOVA using Welch's *t*-test also indicated treatment by silver acetate had little effect on gene expression. Using a stringent criterion of Bonferroni-adjusted $p < 0.05$, the analysis revealed no differentially expressed genes (DEGs) from all treatment groups (vs. controls), whether the analysis was conducted within each gender group or with both gender groups combined. When a less stringent criterion (*p*-value not adjusted for multiple testing, i.e., unadjusted $p < 0.05$) was used for the selection of DEGs, a number of significant genes with fold change (FC) >1.5 were identified in each dose group (Tables 2–4). Treatment with 0.4 mg/kg of silver acetate resulted in 16,

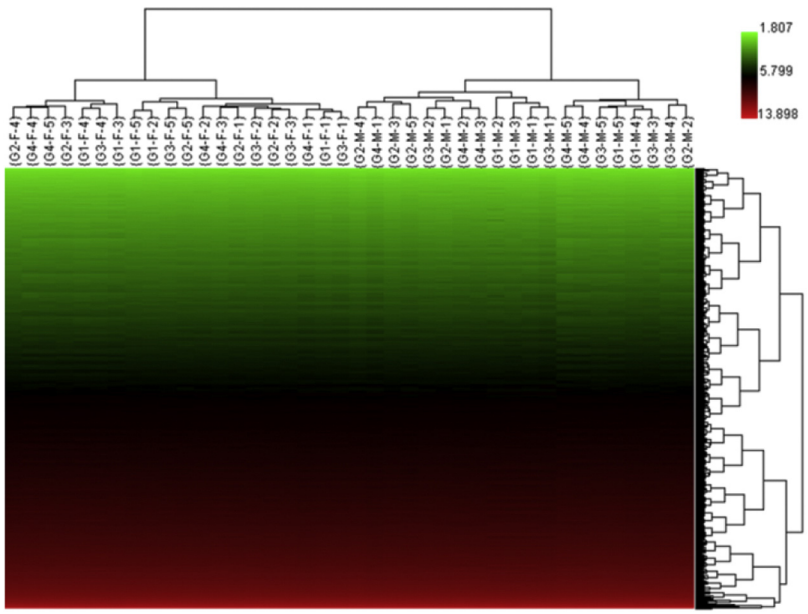

Fig. 2. Hierarchical cluster analysis based on all probe sets in the array to cluster samples based on their similarities or dissimilarities in global gene expression level. The clustering was performed through Ward's minimum variance linkage on normalized expression data which are in $\log_2$ scale and color coded as shown in the scheme at the upper right corner. The tree on the right of the image shows clusters of genes (names not shown), while the tree on the top of the image shows clusters of samples. The naming of the samples follows "group name-gender-replicate"; for example, "G2-F-4" refers to the fourth female pup in group 2. The branches in a tree contain similar samples or genes.

Table 2
Differentially expressed genes in the groups treated with 0.4 mg/kg of silver.[a]

Gene ID	GeneBank Acc. #	Gene name	Description	FC[b]	*p*	FDR[c]
Female (16)						
1369113_at	NM_019282	Grem1	Gremlin 1	0.67	0.036	0.609
1374474_at	BE099085	Cpne8	Copine VIII (predicted)	0.59	0.008	0.572
1378518_at	BF394458	Ewsr1	Regulated endocrine-specific protein 18	0.53	0.010	0.572
1379547_at	AA964652			0.27	0.014	0.590
1380559_at	AI030465		Zic family member 2 (odd-paired homolog, Drosophila) (predicted)	2.73	0.000	0.415
1381670_at	BF412681			1.82	0.047	0.638
1385098_at	AW526343		Sortilin-related VPS10 domain containing receptor 3 (predicted)	0.63	0.008	0.571
1388985_at	AI012869	LOC100361467	Cofilin 2, muscle (predicted)	0.63	0.024	0.607
1389649_at	AI411897			0.66	0.009	0.572
1391830_at	AI059204	Cpne8	Copine VIII (predicted)	0.59	0.006	0.563
1395221_at	AA892908	Snx13	Sorting nexin 13 (predicted)	0.66	0.043	0.626
1395888_at	BF559498			1.61	0.023	0.607
1396019_at	BF419464		Coiled-coil-helix-coiled-coil-helix domain containing 5 (predicted)	1.61	0.036	0.609
1396931_at	AI137091			1.68	0.042	0.622
1397064_at	BE114456			1.56	0.034	0.609
1397730_at	C06959	RGD1307235	Similar to RIKEN cDNA 2310035C23 (predicted)	0.65	0.001	0.560
Male (16)						
1368487_at	NM_021696	Serpinb2	Serine (or cysteine) peptidase inhibitor, clade B, member 2	1.56	0.034	0.376
1370382_at	BI279526	RT1-Db1	RT1 class II, locus Db1	2.20	0.014	0.351
1375562_at	BF408460		Similar to [Mouse primary response gene B94 mRNA, 3end.], gene product	0.66	0.003	0.306
1375758_at	BF404935			0.48	0.048	0.397
1376780_at	AI172311	Fam103a1	Family with sequence similarity 103, member A1	0.39	0.025	0.364
1379435_at	AI599463	Dguok	Deoxyguanosine kinase (predicted)	4.51	0.022	0.354
1385240_at	AW523099	Wdr33	WD repeat domain 33 (predicted)	0.64	0.046	0.395
1388236_x_at	M24026	RT1-CE12	RT1 class I, CE12	0.63	0.048	0.397
1388272_at	AI411947	LOC100363606	Immunoglobulin heavy chain 1a (serum IgG2a)	2.18	0.034	0.375
1391544_at	BI285941		Similar to adiponutrin	0.55	0.047	0.396
1392118_at	BE099845			0.66	0.006	0.331
1392854_at	BE116127	RGD1564560	Similar to RCK (predicted)	1.75	0.011	0.349
1392894_at	AI716194	Fgl2	Fibrinogen-like 2	1.70	0.009	0.349
1393795_at	BG377397	Zeb2	Zinc finger E-box binding homeobox 2	0.61	0.032	0.372
1397064_at	BE114456			1.65	0.003	0.306
1398533_at	BE105837	Cyfip2	Cytoplasmic FMR1 interacting protein 2 (predicted)	0.58	0.012	0.351
All (15)						
1367739_at	NM_012786	Cox8b	cytochrome c oxidase, subunit 8B	0.61	0.044	0.924
1371363_at	BI277042	Gpd1	Glycerol-3-phosphate dehydrogenase 1 (soluble)	0.55	0.039	0.924
1371400_at	AI169092	Thrsp	Thyroid hormone responsive protein	0.55	0.045	0.924
1375758_at	BF404935			0.61	0.016	0.924
1378518_at	BF394458	Ewsr1	Regulated endocrine-specific protein 18	0.66	0.008	0.924
1379547_at	AA964652			0.37	0.005	0.924
1381670_at	BF412681			1.66	0.017	0.924
1382849_at	AA893195			4.15	0.008	0.924
1385380_at	AI044983			0.65	0.009	0.924
1386911_at	NM_012505	Atp1a2	ATPase, Na+/K+ transporting, alpha 2 polypeptide	0.60	0.030	0.924
1388272_at	AI411947	LOC100363606	Immunoglobulin heavy chain 1a (serum IgG2a)	1.78	0.012	0.924
1391544_at	BI285941		Similar to adiponutrin	0.63	0.013	0.924
1393738_s_at	AI136864	Mfhas1	Malignant fibrous histiocytoma amplified sequence 1 (predicted)	0.66	0.039	0.924
1393795_at	BG377397	Zeb2	Zinc finger E-box binding homeobox 2	0.67	0.003	0.924
1397064_at	BE114456			1.60	0.000	0.924

[a] The analysis was conducted within each gender group ("Female" or "Male") or with both gender groups combined ("All"). The number of significant genes in each gender group is included in parentheses following the gender name.
[b] Fold changes relative to the control group.
[c] False discovery rate, which is the probability of having false tests among all the significant tests. For example, an FDR of 0.05 indicates that 5% of the significant genes may have been identified by chance (i.e., the false-positives).

Table 3
Differentially expressed genes in the groups treated with 4.0 mg/kg of silver.[a]

Gene ID	GeneBank Acc. #	Gene name	Description	FC[b]	*p*	FDR[c]
Female (13)						
1368337_at	NM_012794	Glycam1	Glycosylation-dependent cell adhesion molecule 1	0.50	0.012	0.986
1369342_at	NM_052803	Atp7a	ATPase, Cu^{2+} transporting, alpha polypeptide	2.84	0.010	0.986
1372264_at	BI277460	Pck1	Phosphoenolpyruvate carboxykinase 1, cytosolic	0.40	0.025	0.986
1381208_at	BE104595	Hist3h2a	Histone cluster 3, H2a	1.51	0.030	0.986
1381990_at	AA963979		UDP-*N*-acetyl-alpha-D-galactosamine:polypeptide *N*-acetylgalactosaminyltransferase 1	0.66	0.006	0.986
1382849_at	AA893195			4.12	0.049	0.986
1383242_a_at	BF561222			0.56	0.022	0.986
1384372_at	BF545278		Neural precursor cell-expressed, developmentally down-regulated gene 4A	1.52	0.048	0.986
1388985_at	AI012869	LOC100361467	Cofilin 2, muscle (predicted)	0.62	0.012	0.986
1392189_at	BE105136	Rfx4	Regulatory factor X, 4 (influences HLA class II expression)	2.08	0.026	0.986
1393795_at	BG377397	Zeb2	Zinc finger E-box binding homeobox 2	0.44	0.022	0.986
1397463_at	BE105818	Rab14	RAB14, member RAS oncogene family	0.64	0.030	0.986
1397730_at	C06959	RGD1307235	Similar to RIKEN cDNA 2310035C23 (predicted)	0.56	0.001	0.986
Male (9)						
1372927_at	AA891839	Mrpl50	Mitochondrial ribosomal protein L50 (predicted)	0.62	0.001	0.994
1380773_at	BI288767		6-Phosphogluconolactonase (predicted)	1.52	0.014	0.994
1381858_at	BM387283	Trim14	Tripartite motif protein 14 (predicted)	0.67	0.013	0.994
1384136_at	BI291045	Osbpl3	Oxysterol binding protein-like 3	0.66	0.044	0.994
1385635_at	AI029143	Cd5l	CD5 antigen-like	2.17	0.022	0.994
1392012_at	BE100353	LOC686567		0.61	0.043	0.994
1392894_at	AI716194	Fgl2	Fibrinogen-like 2	1.52	0.045	0.994
1393738_s_at	AI136864	Mfhas1	Malignant fibrous histiocytoma-amplified sequence 1 (predicted)	0.53	0.033	0.994
1393795_at	BG377397	Zeb2	Zinc finger E-box binding homeobox 2	0.46	0.038	0.994
All (9)						
1369342_at	NM_052803	Atp7a	ATPase, Cu^{2+} transporting, alpha polypeptide	1.97	0.035	0.909
1370312_at	M88469	Spon1	Spondin 1	0.65	0.038	0.909
1379547_at	AA964652			0.46	0.028	0.909
1382849_at	AA893195			3.10	0.023	0.909
1383242_a_at	BF561222			0.66	0.021	0.909
1385635_at	AI029143	Cd5l	CD5 antigen-like	1.74	0.021	0.909
1392012_at	BE100353	LOC686567		0.65	0.009	0.909
1392189_at	BE105136	Rfx4	Regulatory factor X, 4 (influences HLA class II expression)	1.82	0.020	0.909
1393795_at	BG377397	Zeb2	Zinc finger E-box binding homeobox 2	0.45	0.001	0.896

[a] The analysis was conducted within each gender group ("Female" or "Male") or with both gender groups combined ("All"). The number of significant genes in each gender group is included in parentheses following the gender name.
[b] Fold changes relative to the control group.
[c] False discovery rate, which is the probability of having false tests among all the significant tests. For example, an FDR of 0.05 indicates that 5% of the significant genes may have been identified by chance (i.e., the false-positives).

16, and 15 DEGs for female, male, and combined groups. At 4.0 mg/kg, the numbers of DEGs were 13, 9, and 9 respectively; and at 40.0 mg/kg, the numbers were 14, 12, and 10.

Although the numbers of DEGs did not show dose dependency, the false discovery rate (FDR), which is a statistic (*p*-value) moderately adjusted for multiple testing, were markedly different among different dose groups, and in some cases between different gender groups with the same dose group as well. Remarkably, six probe sets in the male group of the highest dose group (40.0 mg/kg) had an FDR < 0.1 (highlighted in Table 4). Among these probe sets, two are serine/cysteine peptidase inhibitor, namely Serpinb2 and Serpinb3a, one is predicted to be similar to the regulator of K^+ conductance (RCK), another one is an RNA-specific adenosine deaminase and the remaining two are actin binding protein and RNA binding protein, respectively. The heat map shown in Fig. 3 illustrates the differential expression of these genes in the high-dose group (40.0 mg/kg) compared with the control group.

The numbers of DEGs for each treatment or gender group as well as the numbers of overlapping genes are plotted in the Venn diagrams shown in Fig. 4. Within the same dose group (Fig. 4A), it is apparent that different gender groups shared no or very small numbers of genes compared to the total number of changed genes in each gender group, suggesting the gene expression changes were gender-dependent. Similarly, different dose groups

Table 4
Differentially expressed genes in the groups treated with 40.0 mg/kg of silver.[a]

Gene ID	GeneBank Acc. #	Gene name	Description	FC[b]	*p*	FDR[c]
Female (14)						
1368826_at	NM_012531	Comt	Catechol-*O*-methyltransferase	0.32	0.030	0.998
1369342_at	NM_052803	Atp7a	ATPase, Cu^{2+} transporting, alpha polypeptide	2.13	0.021	0.998
1378346_at	AI385237		Similar to IQ motif and WD repeats 1	0.62	0.021	0.998
1379170_at	BF393059			0.66	0.012	0.998
1381613_at	BI290213			0.39	0.020	0.998
1382597_at	BF288069		Formin binding protein 3 (predicted)	0.63	0.001	0.998
1383187_a_at	AA944136		Bol, boule-like (Drosophila) (predicted)	0.59	0.030	0.998
1383242_a_at	BF561222			0.50	0.016	0.998
1383598_at	AI136294	Wdr91	WD repeat domain 91	1.55	0.013	0.998
1384067_at	BF288361			0.40	0.024	0.998
1384126_a_at	AW917217		Cytoskeleton-associated protein 2 (predicted)	0.60	0.004	0.998
1384136_at	BI291045	Osbpl3	Oxysterol binding protein-like 3	1.90	0.011	0.998
1388985_at	AI012869	LOC100361467	Cofilin 2, muscle (predicted)	0.53	0.027	0.998
1392591_at	AI170983	MGC125002	Similar to RIKEN cDNA 5830433M19	0.65	0.002	0.998
Male (12)						
1368487_at*	NM_021696	Serpinb2	Serine/cysteine peptidase inhibitor, clade B, member 2	1.64	0.002	0.073
1370371_a_at	U23056	Ceacam1///Ceacam10	CEA-related cell adhesion molecule 10	0.45	0.014	0.130
1372725_at	AI411594	Plscr2	Phospholipid scramblase 2	1.57	0.047	0.208
1378738_at	BE097574	Kcnab1	Potassium voltage-gated channel, shaker-related subfamily, beta member 1	1.67	0.049	0.213
1378866_at*	BF401176		Actin-binding LIM protein 1	1.85	0.003	0.079
1381839_at	AA957129		Similar to hypothetical protein FLJ13855 (predicted)	0.60	0.027	0.161
1383163_at	AA817898	Igj	Immunoglobulin joining chain	1.52	0.039	0.191
1392854_at*	BE116127	RGD1564560	Similar to RCK (predicted)	2.02	0.006	0.094
1393738_s_at	AI136864	Mfhas1	Malignant fibrous histiocytoma amplified sequence 1 (predicted)	0.54	0.031	0.174
1394585_at*	BE116089		Adenosine deaminase, RNA-specific	0.55	0.000	0.052
1397212_at*	AW534279		Spermatid perinuclear RNA binding protein	0.64	0.001	0.064
1397463_at	BE105818	Rab14	RAB14, member RAS oncogene family	0.50	0.017	0.140
1397635_at*	BM390325	Serpinb3a	Serine (or cysteine) peptidase inhibitor, clade B (ovalbumin), member 3A	1.83	0.004	0.080
All (10)						
1369342_at	NM_052803	Atp7a	ATPase, Cu^{2+} transporting, alpha polypeptide	2.22	0.007	0.228
1370371_a_at	U23056	Ceacam1///Ceacam10	CEA-related cell adhesion molecule 10	0.49	0.002	0.162
1381613_at	BI290213			0.50	0.005	0.204
1383242_a_at	BF561222			0.60	0.022	0.288
1384067_at	BF288361			0.48	0.005	0.204
1384393_at	BE120370		Cln3p	1.63	0.034	0.321
1388985_at	AI012869	LOC100361467	Cofilin 2, muscle (predicted)	0.61	0.005	0.204
1393795_at	BG377397	Zeb2	Zinc finger E-box binding homeobox 2	0.61	0.012	0.256
1394671_at	AI454769		Glucosamine (*N*-acetyl)-6-sulfatase (predicted)	0.60	0.014	0.263
1397463_at	BE105818	Rab14	RAB14, member RAS oncogene family	0.61	0.003	0.171

[a] The analysis was conducted within each gender group ("Female" or "Male") or with both gender groups combined ("All"). The number of significant genes in each gender group is included in parentheses following the gender name.
[b] Fold changes relative to the control group.
[c] False discovery rate, which is the probability of having false tests among all the significant tests. For example, an FDR of 0.05 indicates that 5% of the significant genes may have been identified by chance (i.e., the false-positives).
* Genes with FDR < 0.1.

within the same gender group also had very few overlapped genes compared to the total number of changed genes in each dose group (Fig. 4B), suggesting the gene expression changes were also dose-dependent. However, source of variance (SV) plot from two-way ANOVA on dose and gender (Fig. 5) indicated that gender had a much greater contribution than dose to the gene expression changes.

4. Discussion

With the increasing application of silver-containing compounds as antimicrobial agents in the food industry, it is imperative to study their safety, toxicity, and health effect. The U.S. FDA evaluated data available on the use of silver mixtures as antimicrobial agents in food contact polymers and suspected that *in utero* exposure to silver may have an adverse effect on the immune system of the developing animal. A comprehensive study for risk assessment has been conducted in our group using a rat model and conventional toxicological and/or pathological endpoints to confirm that the previously observed adverse effects are due to silver ion alone and to define the NOEL [16].

As a component of the comprehensive research, the present study used a toxicogenomic approach to study the effect of silver ions on the developing thymus at the

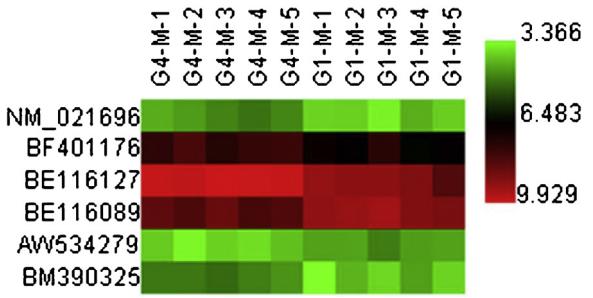

Fig. 3. Heat map showing the differential expression of some genes with FDR < 0.1 in males of the high dose group (40.0 mg/kg, G4) compared with the control group (G1). The data are normalized signal intensity value in $\log_2$ scale and color coded as shown in the scheme at the upper right corner. The naming of the samples follows "group name-gender-replicate"; for example, "G4-M-1" refers to the first male pup in group 4.

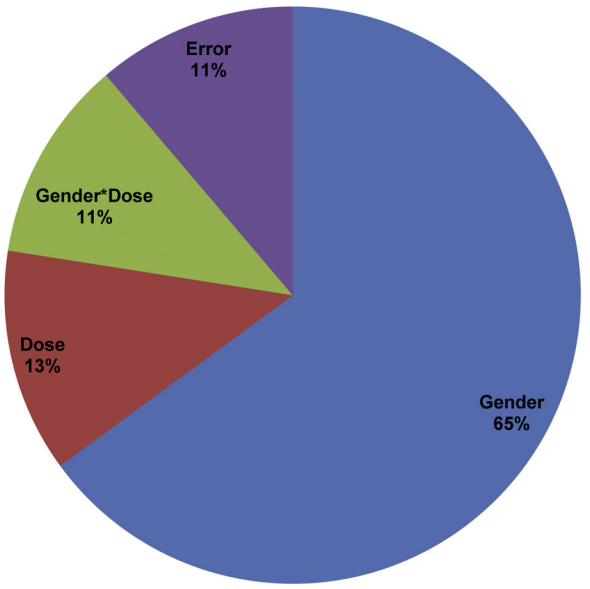

Fig. 5. Source of variance (SV) plot from two-way ANOVAs showing the contribution from gender, dose, their interaction (gender × dose), and error.

transcriptional level. Global gene expression profile in rat thymus of F1 generation pups at postnatal day 26 following maternal exposure to silver acetate at 0, 0.4, 4.0, or 40.0 mg/kg in drinking water are reported here. Unsupervised data exploration by PCA (Fig. 1) and HCA (Fig. 2) revealed that the samples were separated by gender into two major clusters. Within each gender group, however, no distinct expression patterns were identified for different dose groups, suggesting treatment by silver acetate had little effect on global gene expression. Consistently, one-way ANOVA identified only about a dozen DEGs in each dose group with FC > 1.5 and unadjusted $p < 0.05$, and none of these genes had an FDR <0.05 (Tables 2–4). Six genes had an FDR < 0.1 in the males of the highest treatment group (Table 4); however, visual inspection of the heat map suggests these genes are likely false-positives (Fig. 4). Taken together, these results indicate silver acetate up to 40.0 mg/kg did not affect gene expression in the developing thymus.

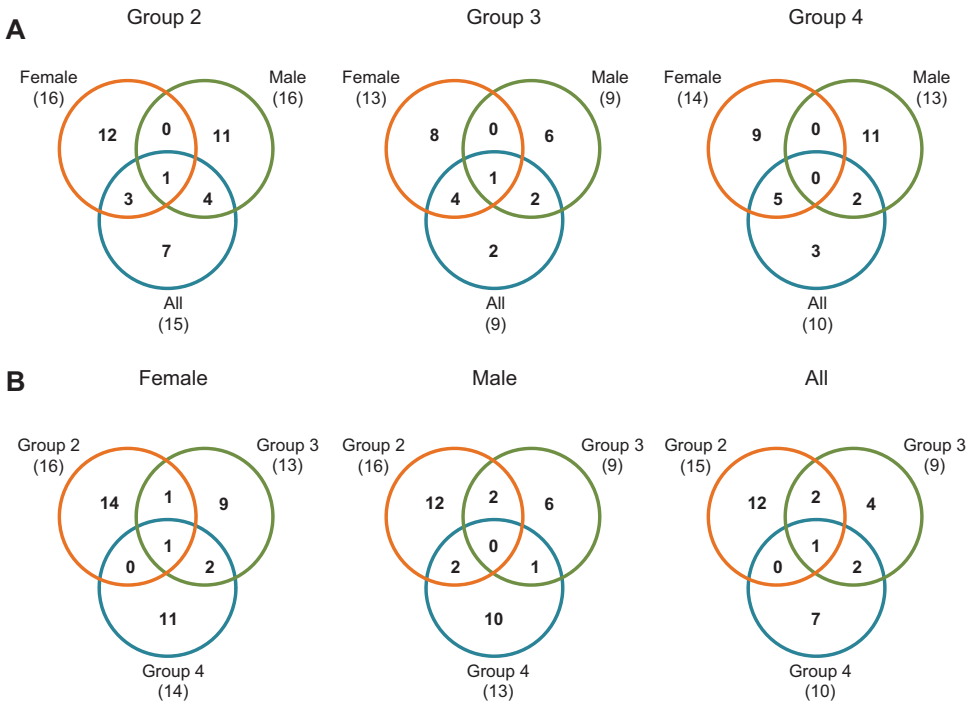

Fig. 4. Venn diagrams showing overlap of differentially expressed genes (DEGs) between different gender groups in the same dose group (A) and between different dose groups in the same gender group (B). The total number of DEGs in each group is included in the parentheses under the group name.

In the large-scale study, no histopathological abnormalities in thymus were identified in the F1 generation pups in any of the dosing groups [16]. Combined with the observation that thymus-to-body-weight ratios were not affected (Table 1), the current study suggests that *in utero* exposure to silver ions up to 26.0 mg/kg (equivalent to 40.0 mg/kg silver acetate) did not have an adverse effect on the developing thymus.

A parallel component study [19] on natural killer (NK) activity and mitogen-induced lymphocyte proliferation in the spleen of the F1 generation pups has found that maternal exposure to 4.0 and 40.0 mg/kg silver acetate resulted in reduced T-cell development and cell-mediated immune functions in 4-day pups, and reduced TCR+ cells and cell-mediated immune functions in 26-day-old pups, although exposure to low concentration of silver acetate (0.4 mg/kg) has slight beneficial effect on NK activity in 26-day pups. In contrast, no effect was observed on thymic lymphocytes. Hultman et al. [7] found that Brown Norway (BN) rats exposed to silver in dental amalgam restorations had significantly increased metal (including silver) concentrations in tissue in the order kidney > spleen > cerebrum occipital lobe > cerebellum > liver > thymus. For example, mercury concentration in spleen is more than 30-fold higher than that in thymus. Silver accumulation may follow the same pattern as mercury. This may partly explain the results of [19] that silver acetate had a significant impact on the splenic but not thymic immune system and may also help to explain the findings of the current study that silver acetate had not significant effect on thymic gene expression.

It should be noted that silver ions may exert systemic effects on the developing pups that are not evident in specific organs. McIntyre et al. [10] reported that a 12-month infant overdosed with colloidal silver in the form of dietary supplements manifested global developmental retardation, although this case was complicated by malnutrition. In the comprehensive study [16], higher runt numbers and low average body weights were observed in pups following maternal exposure to silver acetate at high concentrations (4.0 and 40.0 mg/kg). In addition, prenatal death rate of newborns was also higher in dams exposed to high concentrations (4.0 and 40.0 mg/kg) of silver acetate.

5. Conclusions

In the present study, we used a toxicogenomic approach to study the effect of silver ions on the developing thymus by measuring transcriptome changes in rat thymus of F1 generation pups following maternal exposure to silver acetate. Gene expression profiling analyses indicate that silver acetate up to 40.0 mg/kg did not affect gene expression in the developing thymus. Combined with the observation that thymus-to-body-weight ratios were not affected, and no histopathological abnormalities in thymus were identified in the pups, the current study suggests that *in utero* exposure to silver ions up to 26.0 mg/kg (equivalent to 40.0 mg/kg silver acetate) did not have an adverse effect on the developing thymus.

Acknowledgements

The authors thank Isha Patel, Jayanthi Gangiredla, and Scott Jackson for their help with the microarray experiment. This research is funded by internal funds of the U.S. Food and Drug Administration. X.G. and V.D.T. were supported by an appointment to the Research Participation Program at the Center for Food Safety and Applied Nutrition administered by the Oak Ridge Institute for Science and Education (ORISE) through an interagency agreement between the U.S. Department of Energy and the U.S. Food and Drug Administration. The findings and conclusions presented in this article are solely those of the authors and do not necessarily represent views, opinions, or policies of the U.S. Food and Drug Administration.

Appendix A. Supplementary data

Supplementary data associated with this article can be found, in the online version, at doi:10.1016/j.toxrep.2014.12.008.

References

[1] A. Aschengrau, S. Zierler, A. Cohen, Quality of community drinking water and the occurrence of late adverse pregnancy outcomes, Arch. Environ. Health 48 (1993) 105–113.
[2] V. Edwards-Jones, The benefits of silver in hygiene, personal care and healthcare, Lett. Appl. Microbiol. 49 (2009) 147–152.
[3] M.B. Eisen, P.T. Spellman, P.O. Brown, D. Botstein, Cluster analysis and display of genome-wide expression patterns, Proc. Natl. Acad. Sci. U.S.A. 95 (1998) 14863–14868.
[4] C. Elliott, The effects of silver dressings on chronic and burns wound healing, Br. J. Nurs. 19 (2010) S32–S36.
[5] H.K. Hamadeh, R.P. Amin, R.S. Paules, C.A. Afshari, An overview of toxicogenomics, Curr. Iss. Mol. Biol. 4 (2002) 45–56.
[6] S. Hochreiter, D.A. Clevert, K. Obermayer, A new summarization method for Affymetrix probe level data, Bioinformatics 22 (2006) 943–949.
[7] P. Hultman, U. Lindh, P. Hörsted-Bindslev, Activation of the immune system and systemic immune-complex deposits in Brown Norway rats with dental amalgam restorations, J. Dent. Res. 77 (1998) 1415–1425.
[8] R.A. Irizarry, B. Hobbs, F. Collin, Y.D. Beazer-Barclay, K.J. Antonellis, U. Scherf, T.P. Speed, Exploration, normalization, and summaries of high density oligonucleotide array probe level data, Biostatistics 4 (2003) 249–264.
[9] G.A. Leblanc, J.D. Mastone, A.P. Paradice, B.F. Wilson, H.B. Lockhart Jr., K.A. Robillard, The influence of speciation on the toxicity of silver to fathead minnow (*Pimephales promelas*), Environ. Toxicol. Chem. 3 (1984) 37–46.
[10] E. McIntyre, J. Wilcox, J. McGill, P.J. Lewindon, Silver toxicity in an infant of strict vegan parents, J. Pediatr. Gastroenterol. Nutr. 33 (2001) 501–502.
[11] B. Nowack, H.F. Krug, M. Height, 120 years of nanosilver history: implications for policy makers, Environ. Sci. Technol. 45 (2011) 1177–1183.
[12] A. Oberemm, L. Onyon, U. Gundert-Remy, How can toxicogenomics inform risk assessment? Toxicol. Appl. Pharmacol. 207 (2 Suppl) (2005) 592–598.
[13] H.C. Poynton, J.M. Lazorchak, C.A. Impellitteri, B.J. Blalock, K. Rogers, H.J. Allen, A. Loguinov, J.L. Heckman, S. Govindasmawy, Toxicogenomic responses of nanotoxicity in *Daphnia magna* exposed to silver nitrate and coated silver nanoparticles, Environ. Sci. Technol. 46 (2012) 6288–6296.
[14] M. Ringnér, What is principal component analysis? Nat. Biotechnol. 26 (2008) 303–304.
[15] T. Shioda, Application of DNA microarray to toxicological research, J. Environ. Pathol. Toxicol. Oncol. 23 (2004) 13–31.
[16] R.L. Sprando, T. Black, Z. Keltner, N. Olejnik, M. Ferguson, Low dose silver acetate exposure: effects on reproduction and post natal development, Food Chem. Toxicol. (2015) (in review).

[17] W. Tong, X. Cao, S. Harris, H. Sun, H. Fang, J. Fuscoe, A. Harris, H. Hong, Q. Xie, R. Perkins, L. Shi, D. Casciano, ArrayTrack-supporting toxicogenomic research at the U.S. Food and Drug Administration National Center for Toxicological Research, Environ. Health Perspect. 111 (2003) 1819–1826.
[18] W. Tong, S. Harris, X. Cao, H. Fang, L. Shi, H. Sun, J. Fuscoe, A. Harris, H. Hong, Q. Xie, R. Perkins, D. Casciano, Development of public toxicogenomics software for microarray data management and analysis, Mutat. Res. 549 (2004) 241–253.
[19] U.S. Babu, K.V. Balan, E. Bigley, M. Pereira, T. Black, N. Olejnik, Z. Keltner, R.L. Sprando, Effects of maternal silver acetate exposure on immune biomarkers in a rodent model, Food Chem. Toxicol. (2015) (in review).
[20] P.A. Walker, P. Kille, A. Hurley, N.R. Bury, C. Hogstrand, An in vitro method to assess toxicity of waterborne metals to fish, Toxicol. Appl. Pharmacol. 230 (2008) 67–77.
[21] M.Y. Wu, K. Suryanarayanan, W.J. van Ooij, D.B. Oerther, Using microbial genomics to evaluate the effectiveness of silver to prevent biofilm formation, Water Sci. Technol. 55 (2007) 413–419.